PIBB 生物化学与生物物理进展
Progress in Biochemistry and Biophysics
2007, 34(5): 479~489
www.pibb.ac.cn

Homocysteine-mediated Aberrant DNA Methylation in Vascular Smooth Muscle Cells and Its Potential Pathogenic Mechanism*

JIANG Yi-Deng[1], ZHANG Jian-Zhong[2], HUANG Ying[1], SU Juan[1],
ZHANG Jing-Ge[1], WANG Li-Zhen[1], HAN Xiao-Qun[1], WANG Shu-Ren[1]**
([1]*Department of Pathophysiology, West China College of Preclinical and Forensic Medical Sciences, Sichuan University, Chengdu* 610041, China;
[2]*Department of Pathology, Ningxia Medical College, Yinchuan* 750004, China)

Abbreviations: SAH, S-adenosylhomocysteine; SAM, S-adenosylmethionine; C-5MT-ase, C-5 DNA methyltransferase; gDNA, global DNA; Hcy, homocysteine; SAHH, SAH hydrolase; VSMCs, vascular smooth muscle cells; HHcy, hyperhomocysteinemia; MTT, 3-(4,5-dimethyl-2-thiazolyl)-2,5-diphenyl-2H-tetrazolium-bromide

Abstract Hyperhomocysteinemia, which is an independent risk factor for atherosclerosis, may cause aberrant methylation and dysregulation of gene expression, but the characteristics of the aberrant methylation and its key links involved in its pathogenic mechanisms are still poorly understood. The effect of hyperhomocysteine on DNA methylation in vascular smooth muscle cells, its characteristics and the underlying mechanism of Hcy-induced changing in DNA methylation patterns were investigated. Clinical relevant concentrations of homocysteine was added into the cultured vascular smooth muscle cells of the *Homo sapien* umbilical vein for 24 h. The level of SAM and SAH was detected by HPLC. The activity of SAH Hydrolase was detected by real-time quantitative reverse transcription-PCR and Western blotting analysis. The level and patterns of DNA methylation were measured by endogenous C-5 DNA methyltransferase(C-5 MT-ase) activity and capacity of genomic DNA to accept methy1 groups and methylation-dependent restriction analysis. The results indicated that an increased Hcy concentration induced elevated SAH, declined SAM and the ratio of SAM/SAH, reduced expression of SAH Hydrolase, but increased activity of C-5MT-ase. The methylation status of gDNA analyzed by methyl-accepting capacity of gDNA uncovered a demethylation process in gDNA, or homocysteine-caused hypomethylation in gDNA. With different methylation-dependent restriction endonucleases, the aberrant demethylation was found to prefer C↓CGG sequences to CpG islands. The impacts of different dosage of Hcy showed that the varied detrimental effects of Hcy could be attributed to different concentrations via different mechanisms. In mild and moderate hyperhomocysteinemia, the Hcy may primarily influence the epigenetic regulation of gene expression through the interference of transferring methyl-group metabolism, while in more higher Hcy concentration, the notorious impacts may be more directly caused *via* oxidative stress, apoptosis, inflammation etc.

Key words homocysteine, DNA methyltransferase, DNA methylation, SAM, SAH hydrolase

Homocysteine (Hcy) is a sulfur-containing amino acid formed during the metabolism of methionine. Mounting evidences have indicated that elevated plasma Hcy levels is a common and independent risk factor for cardiovascular disorders [1~4] and strong association between hyperhomocysteinemia and atherosclerosis has been observed in many retrospective and prospective studies [5]. However, the precise mechanisms of homocysteine-inducing atherosclerosis remain obscure up to date.

Atherosclerosis is a complex disease characterized by accumulation of lipids, fibrous materials, cell debris, and minerals in the intima of arteries [6]. Much attention has been focused on characterizing the impacts of hyperhomocysteine on dysfunction and injury of vascular cells. Increasing evidence, however, indicate that HHcy may also be involved in disturbing the expression of atherosclerosis-related genes through the interference

*This work was supported by a grant from Specialized Research Fund for The Doctoral Program of Higher Education, China (20050610050).
**Corresponding author .
Tel: 86-28-85501268, E-mail: wangshuren1945@yahoo. com.cn
Received: October 23, 2006 Accepted: December 6, 2006

of DNA methylation[7,8].

The methylation of cytosine located within the cytosine-guanine (CpG) dinucleotide sequences is a heritable, tissue-specific, epigenetic modification of mammalian genomic DNA[9,10]. Hypomethylation is an early and consistent event in the development of several cancers, and is associated with advanced human atherosclerotic lesions. Some reports have shown recently that genomic hypomethylation is present in lesions of apolipoprotein E (ApoE) knockout mice and neointima of balloon-denuded New Zealand White (NZW) rabbit aortas[11], and also shown that significant genomic hypomethylation develops during the first replication of aortic SMCs *in vivo*, and that hypomethylation occurs in some specific genes, such as 15-lipoxygenase and extracellular superoxide dismutase, which have been indicated a deep involvement in atherosclerosis[12,13]. Estrogen receptor gene, the factor shown protective role against atherosclerosis however, was found to be hypermethylation in atheromas compared with normal aorta[14,15], and it was also shown to be methylated in SMCs *in vitro* during the phenotypic switch[16].

How can HHcy interfere DNA methylation? And what pathway does this interference go through? So the aim of the present studies is to investigate the effects of hyperhomocysteinemia (HHcy) on the activity of SAHH which hydrolyzes the SAH to homocysteine and on the C-5 MT-ase which transfers the methyl group to DNA, as well as their correlations with the methylation status of CpG sequences in DNA. The uncovered aberration of DNA methylation and its pathways could be a potential target for anti-atherosclerosis. The alteration of DNA methylation may be an important findings which may point to a mechanism against atherosclerosis in which epigenetic gene silencing is a feature. These data,for the first time, indicate the effect of DNA methylation of the Hcy in the context of atherosclerosis.

1 Methods

1.1 Chemicals

SAM,SAH,homocysteine(Hcy), poly[dI-dC]. poly [dI-dC] and [methyl-^{3}H] SAM were purchased from Sigma Aldrich Chemical Co; restriction endonucleases *Hpa* Ⅱ and *Bss*H Ⅱ were products of Promega; *Sss* Ⅰ methylase (CpG methylase) was product of New England BioLabs.

1.2 Cell culture and treatment of Homo sapien umbilical vein smooth muscle cell

Primary culture of VSMCs was obtained from the media of the umbilical vein of *Homo sapien*. The cells were grown in Dulbecco's modified eagle's medium-Ham's F12 media(DMEM-F12, Gibco BRL) supplemented with 20% Fetal calf serum (FCS), 100 U/ml penicillin and 100 U/ml streptomycin.The culture was harvested in 25 cm^2 culture flask which was in a incubator containing 5% CO_2 at 37℃. At the following passage, cells were planted into 6-well plates. When cells grew to 80% confluence, serum was deprived for 24 h to reach synchronous, then with 5% fetal calf serum for another 24 h before homocysteine addition. Homocysteine was applied at the concentrations of 0 (control), 50, 100, 200 and 500 μmol/L, respectively in order to compensate for the short half-life of homocysteine, which was replenished every 8 h (total three times).

1.3 Cell viability test

Methylthiazoletetrazolium (MTT, Sigma) was used for evaluation of cell viability. The assay detects living but not dead cells. Cells were grown in 96-well microtiter plates at 10^4 cells in 200 μl/well. After cells were incubated to confluence, homocysteine was added at above-mentioned concentrations and incubated for 24 h. Homocysteine was replenished every 8 h. Then, 20 μl MTT (5 g/L) was added to each well and incubated at 37℃ for 4 h. All the supernatant was pipetted off and 150 μl of DMSO was added to each well. After 10 min of incubation at room temperature, plates were read on a micro-enzyme linked immunosorbent assay reader at 490 nm. Values were normalized by control value.

1.4 High-performance liquid chromatography (HPLC) : SAM and SAH

SAM and SAH were determined by use of the method of reversed-phase high-performance liquid chromatography based on a modification of Fell D's describing procedure[17]. The SAM and SAH standards were dissolved in water at a concentration of 1 mmol/L and then diluted with 0.4 mol/L $HClO_4$ to the final concentrations used for HPLC analysis. 25 μl of standard solution containing 50～11 000 pmol was injected into HPLC for preparation of standard curve.

The cells (2×10^7) were centrifuged and washed with cold phosphate-buffered saline (PBS) twice, and kept on the ice. PBS was carefully aspirated and the cell pellets were resuspended in 300 μl 0.4 mol/L

ice-cold perchloric acid ($HClO_4$). The cell pellets were hand-homogenized on ice with a hand-held mini pestle. Homogenates were centrifuged at 10 000 *g* for 10 min at 4℃ and the supernatants were collected and stored at −70℃ until they were analyzed. The supernatant of each sample was filtered through 0.45 μmol/L (millipore) and then was loaded into a C18 column (250 mm×4.6 mm I.D, 5 μm particle) (Clifton, NJ, USA) fitted with a matched guard column, run by a Waters HPLC system (Milford, MA, USA) and connected to an ultraviolet detector. Absorption of eluted compounds was monitored at $[lambda]_{ex}$=254 nm. A two-buffer elution system was used: mobile phase A and B, both contain 10 mmol/L ammonium formate and 4 mmol/L 1-heptanesulfonic acid (pH 4). Mobile phase B contains 50% acentonitrile by volume. Elution of SAM and SAH was achieved at a flow rate of 1 ml/min with the following parameters: 0～0.5 min, 100% A; 0.5～20 min, linear gradient to 75% A and 25% B; 20～30 min, 25% B; 30～45 min, 100% A. Chromatograms were recorded by a Hewlett-Packard HP3394 integrator with its quantification accomplished by automatic peak area integration. SAM and SAH standards were used to identify the elution peaks. SAM and SAH values were normalized to cellular protein content that was determined by using the Coomassie brilliant blue method [18]. All analyses were performed in triplicate.

1.5 Real-time quantitative reverse transcription-PCR: SAH hydrolase

Genomic RNA was isolated from the cultured cells by the E.Z.N.A Tissue RNA Kit (Omega Bio-tek), then purified by E.Z.N.A Cycle-pure Kit (Omega Bio-tek). Primers of SAHH gene (GenBank, NM000687) were designed with Primer Premier 5.0 software. The forward primer was 5′ TCACCAAG-AGCAAGTTTGACA 3′ and the reverse primer was 5′ GGAGTCCCTCATAGATGGCATCA 3′. BLASTN was conducted to search the nonredundant set of the GenBank sequence database in order to confirm the total gene specificity of the chosen nucleotide sequences as well as the absence of DNA polymorphisms. Probe primer was 5′ 6-FAM-ATCACCATAGCCTGCTACCA-TAMRA 3′. RNA was reversely transcribed by Revert Aid™ Frist Strand cDNA Synthesis Kit(MBI) in a final volume of 20 μl containing 5 μl RNA, 3 μl oligo dT primer, and 12 μl DEPC-treated water. Incubate at 70℃ for 10 min, then put on the ice. Add 4 μl 5 × reaction buffer, 1 μl Ribonuclease Inhibitor (recombinant) (20 U/μl)，2 μl dNTP mix, 1 μl RevertAid™ M-MuLV Reverse Transcriptase (200 U/μl) to incubate at 20℃ for 10 min, and then incubate at 48℃ for 60 min, cDNA can be frozen for later use or used immediately for PCR.

The real-time PCR was performed by using an iCycler iQ realtime PCR detection system (Bio-Rad) with the program running for 40 cycles at 95℃ for 45 s, 60℃ for 60 s and 72℃ for 120 s. The melting curve analysis was performed at the range 55～95℃ by monitoring 6-FAM fluorescence with increasing temperature of 0.5℃ increment changes at 10 s intervals. PCR-specific products were determined by clear single peak at the melting curves more than 80℃. The specificity of primers was also confirmed as a single band with the correctly amplified fragment size through an agarose gel electrophoresis of the real-time reverse transcription-PCR products. Real-time PCR was duplicated for each cDNA sample. Each gene RNA level was acquired from the value of the threshold cycle (C_t) of the real-time PCR related to that of GAPDH (calibrator) through the formula ΔC_t ($\Delta C_t = C_t(\text{GAPDH}) - C_t(\text{gene of interest})$). Final results were expressed as N-fold differences in target gene expression relative to the calibrator, termed "Ntarget" were determined as follows: $N_{SAHH} = 2^{\Delta C_t(\text{sample}) - 2\Delta C_t(\text{calibrator})}$ where ΔC_t values of the calibrator and sample were determined by subtracting the C_t value of the target gene from the C_t value.

1.6 SAH hydrolase Western blotting analysis

Cultured cells were harvested by scraping with a plastic scraper. Extracts of whole cells (5×10^6) were isolated from cell culture by lysis buffer containing 20 mmol/L HEPES, pH 7.2, 25% glycerol, 0.42 mol/L NaCl, 1.5 mmol/L $MgCl_2$, 0.2 mmol/L EDTA, 0.5 mmol/L DTT, 0.5 mmol/L phenylmethyl sulfonylfluoride (PMSF) and a protease inhibitor cocktail (10 ml/L; Sigma-Aldrich). Protein concentrations were determined by Coomassie Protein Assay. Polyacrylamide gel electrophoresis (7%～19% polyacrylamide gradient gels) was followed by electrophoretic transfer of proteins from the gel to nitrocellulose membrane. The membrane was incubated in 10 ml of blocking solution (0.1 ml/cm^2) for 2 h at room temperature with gentle agitation on a platform shaker, and washed 3 times for 5 min/time in

TBST (50 mmol/L Tris-HCl pH7.6, 150 mmol/L NaCl, 0.05% Tween-20). The membrane was then incubated with a monoclonal anti-SAH Hydrolase antibody (at 1 ∶250 dilution) in 10 ml Primary Antibody Dilution Buffer with gentle agitation for overnight at 4℃, then washed three times with TBST, and incubated with a second antibody (goat anti-rabbit HRP-conjugated IgG, Jackcon Immunoreserch) in PBS at 1 ∶2 000 dilution containing 1% BSA (New England Biolabs) for 1 h at room temperature. After being washed again three times with TBST, the membrane was then incubated with 10 ml LumiGLO with gentle agitation for 1min at room temperature and drained out excess developing solution, but not let it dry, wrapped in a plastic wrap and exposed to X-ray film.

1.7 Endogenous C-5 DNA methyltransferase (C-5 MT-ase) activity

A modification of the assay developed by Adamas *et al*.[19] was used to determine DNA MTase activity. 1×10^6 VSMCs were homogenized by a glass pestle containing 500 μl lysis buffer (100 mmol/L NaCl, 10 mmol/L Tris-HCl, pH 8.0, 25 mmol/L EDTA, 0.5% SDS, proteinase K 0.2 g/L). The suspension was frozen to −70℃, and then thawed to 37℃ with the feeze-thaw cycle for 3 times. Protein was measured by Seamark's method with Coomassie brilliant blue reagen[18]. And all homogenates of the VSMCs were stored at −70℃ before analysis. The reaction mixture which contained cell homogenates(5 μg protein), poly [dI-dC].poly[dI-dC] (0.25 μg) and 11.1×10^{10} μBq of [methyl-^{3}H] SAM in a total volume of 20 μl, was incubated at 37℃ for 2 h. And RNA was removed by adding 20 μl RNase A(25 g/L) at room temperature for 5 min incubation. The DNA was purified by E.Z.N. A Cycle-pure Kit, and purified gDNA was spotted onto Whatman GF/C filter disc, dried at 80℃ for 5 min and counted in the scintillation counter(1600TR Packard Instrument Comp) for determination of C-5 MTase activity. Each reaction was performed triplicate and the assay was repeated three times to blind the source of the samples. For exclusion of background protein, all samples were initially assayed with control containing the whole cell lysate but without poly [dI-dC].poly [dI-dC]. Results were expressed as dpm/μg protein.

1.8 DNA methy1-accepting capacity with the methylation-sensitive restriction analysis

The capacity of gDNA to accept methy1 groups in the presence of exogenous bacterial *Sss* Ⅰ methylase is inversely proportional to the initial DNA methylation status. So the method[20~22] was used to estimate the methy1-accepting capacity of gDNA measured as the loss of unmethylated cytosine after gDNA was digested with methylation-sensitive endonucleases. Two restriction endonucleases, which recognize unmethylated cytosine, were used: *Hpa* Ⅱ, specific for C↓CGG sequences and *Bss*H Ⅱ which digests CpG rich islands (C↓GCGCG). Purified gDNA (5 μg), isolated from the VSMCs, was digested overnight with 10-fold excess *Hpa* Ⅱ or *Bss*H Ⅱ according to the manufacturer's protocols (New England Biolabs, Beverly, MA). Samples of undigested gDNA served as controls. Then the digested and undigested gDNA were treated with E.Z.N.A Cycle-pure Kit and purified gDNA (0.5 μg) was used for DNA methyl-accepting capacity assay as following: purified gDNA (0.5 μg), bacterial *Sss* Ⅰ methylase (2 U) and [methyl-^{3}H]SAM (3 Bq per sample) were incubated in buffer containing 50 mmol/L NaCl,10 mmol/L Tris-HCl, pH 8.0, 10 mmol/L EDTA (final volume 25 μl) for 2 h at 37℃. The reaction was stopped by placing tubes on the ice. Then 25 μl aliquots from each reaction mixture were applied onto GF/C filter discs, counting in the scintillation counting. The results are expressed as [methyl-^{3}H] incorporation/0.5 μg DNA.

1.9 Statistical method

Results are expressed as $\bar{x}\pm s$. The number of experimental samples used in each group is presented in the Figure legends. The data were analyzed using one-way ANOVA and additional analysis using the Student Newman-Keuls test for multiple comparisons within treatment groups or *t* test for between two groups. $P < 0.05$ was considered significant.

2 Results

2.1 Effects of homocysteine on cell viability

Nontreated VSMCs in confluence showed their typical elongated ribbon or spindle-shaped appearance and parallel arrays showed the characteristic "hill and valley" pattern. Addition of 50 μmol/L homocysteine, slightly increased the number of viable cells to (111.6 ± 2.9) % ($P < 0.05$), but as doses increased, MTT test showed a decreased cell viability. Addition of 100 μmol/L, 200 μmol/L and 500 μmol/L of homocysteine resulted in descending cell count on a dose-dependent manner with signs of morphologic

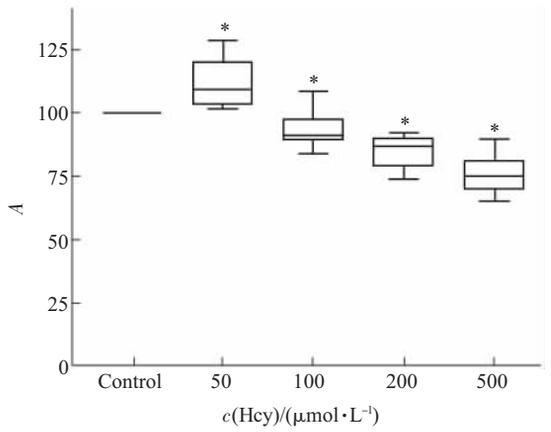

Fig. 1 Homocysteine (Hcy) effect on cell viability evaluated by methylthiazoletetrazolium (MTT) assay in VSMCs

Values for each experiment were converted to percentages related to the corresponding control group (100%). Data expressed as $\bar{x} \pm s$, n=10. Measurements are as described in materials and methods. *P <0.05.

deterioration: the VSMCs became deformed and lost their typical spindle-shaped appearance and some cells appeared swollen and detached from culture plates. 100 μmol/L, 200 μmol/L and 500 μmol/L of homocysteine reduced the viable cell count to (95.02 ± 2.70)% , (84.62 ± 1.90)% , and (75.52 ± 2.90)% (Figure 1).

2.2 Levels of SAM and SAH

SAM and SAH concentrations are important impact factors in the transmethylation process.The intracellular levels of SAH in experimental groups were significantly higher, up to 2- to 3-fold than the control group. The concentrations of SAM and the ratio of SAM/SAH were lower than the control group as Hcy concentration increasing and the ratio of SAM/SAH was even 3- to 4-fold decreased in all experimental groups (Figure 2)

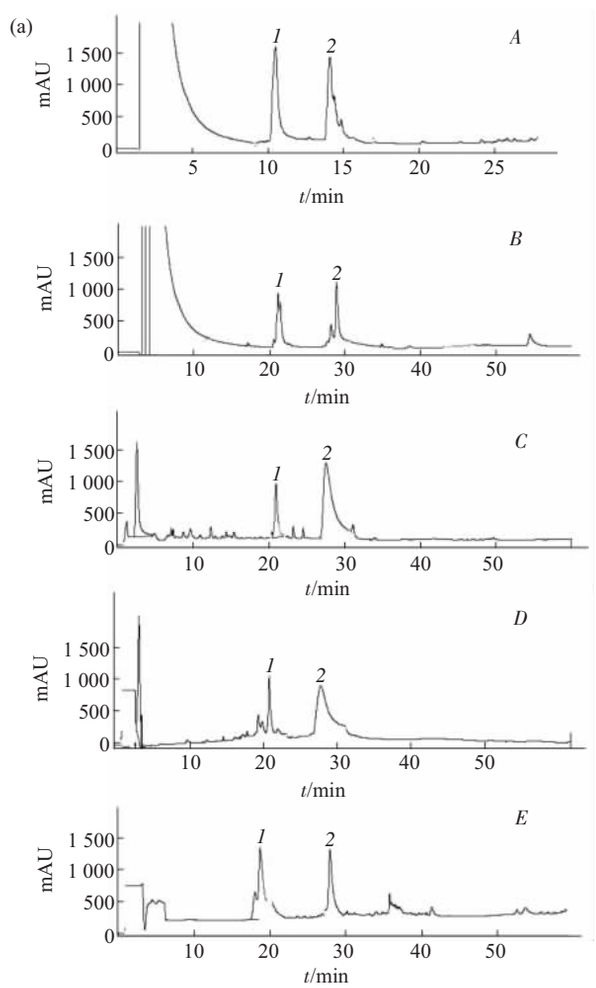

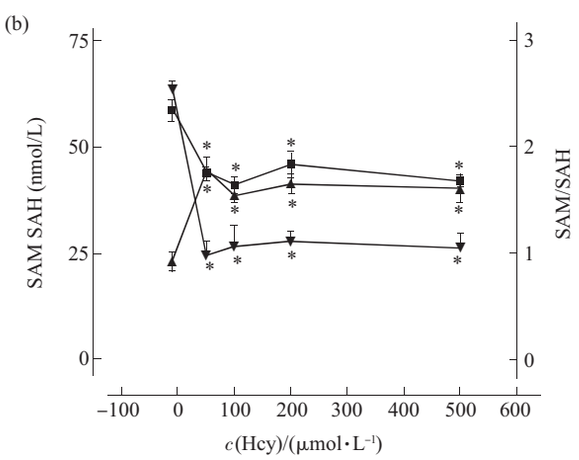

Fig. 2 Homocysteine (Hcy) effect on SAM and SAH concentrations in VSMCs

(a) A chromatogram of SAH and SAM of all groups. *A*: 0 μmol/L Hcy; *B*: 50 μmol/L Hcy; *C*:100 μmol/ L Hcy; *D*: 200 μmol/ L Hcy; *E*: 500 μmol/ L Hcy. Peaks: *1*=SAM, *2*=SAH. The VSMCs was homogenized in four volumes of 0.4 mol/L $HClO_4$. A 200 μl aliquot of the acid extract was applied directly onto the HPLC. Chromatograms were recorded by an integrator. (b) Elevation of SAM,SAH and decreased SAM/SAH ratio. Effects of Hcy on SAH, SAM and SAM/SAH in VSMCs. Quantification of SAM, SAH was accomplished by automatic peak area integration. SAM and SAH standards were used to identify the elution peaks. Results were $\bar{x} \pm s$ for three times. *Significant difference compared with control group P<0.05. ■—■: SAM; ▲—▲: SAH; ▼—▼: SAM/SAH.

2.3 SAH hydrolase mRNA and protein expression analysis

Figure 3a shows the results from real-time RT-PCR, and Figure 3b shows the relative mRNA levels of SAHH after normalization with the signal of GAPDH. The data indicates that the mRNA level of SAHH was down-expressed in all Hcy-treated groups compared with control group ($P < 0.05$), and the lowest expression was at the Hcy concentration of 50 μmol/L, which was 4.5-fold lower than that of control group. But the increasing concentrations of Hcy did not result in a dose-dependent decreasing effects on mRNA level of SAHH, there was no significant difference of mRNA expression of SAHH between the experimental groups.

The effects of Hcy on protein level of SAHH was measured by Western blot (Figure 4a, 4b), which showed a result similar to the mRNA expression of SAHH. The lowest protein expression of SAHH was also at the 50 μmol/L of Hcy concentration, and there was no significant difference of SAHH protein levels in various dosage of Hcy.

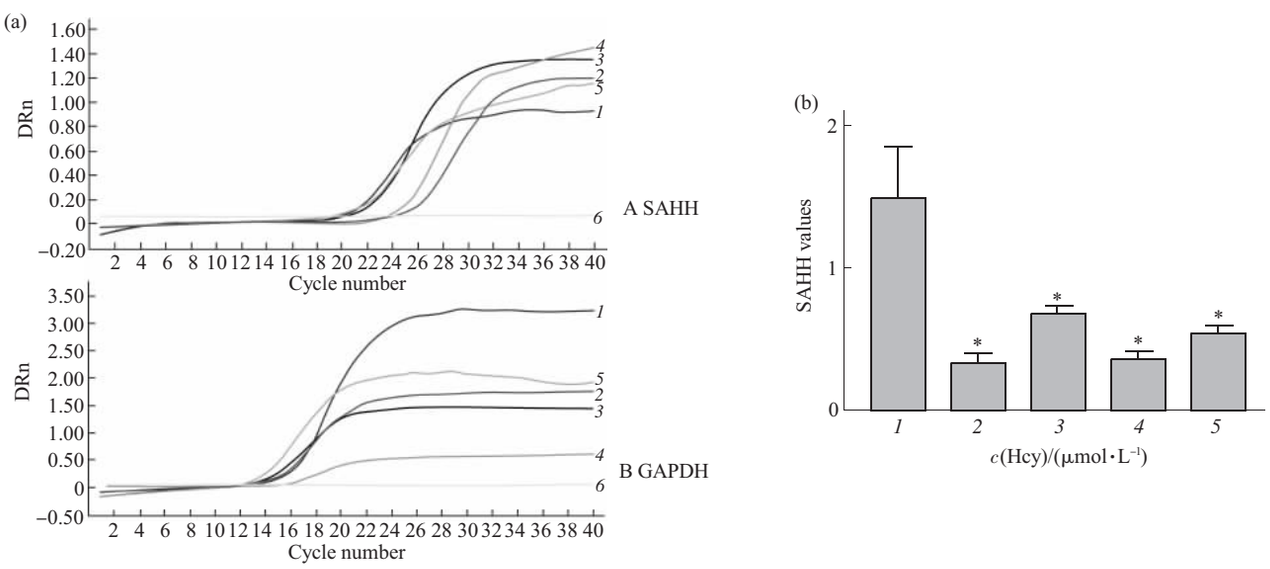

Fig. 3 SAHH and GAPDH real-time RT-PCR graph and effects of homocysteine (Hcy) on SAHH RNA levels in VSMCs

(a)Real-time PCR graph of SAHH and GAPDH. The fluorescence was plotted versus the PCR cycle number for both reactions and each sample dilution was indicated. *1*: Normal; *2*: 50 nmol/L; *3*: 100 nmol/L; *4*: 200 nmol/L; *5*: 500 nmol/L; *6*: Threshold. (b)Relative mRNA levels of SAHH after normalization.Each gene RNA level was acquired from the value of the threshold cycle (C_t) of the real-time PCR as related to that of GAPDH through the formula ΔC_t ($\Delta C_t = C_t$(GAPDH)$-C_t$(gene of interest)).Final results, expressed as N-fold differences in target gene expression relative to the calibrator, termed "N_{target}" is determined as following: $N_{SAHH}=2^{\Delta C_t(\text{sample})-2\Delta C_t(\text{calibrator})}$, where ΔC_t values of the calibrator and sample were determined by subtracting the C_t value of the target gene from the C_t value. Data shown were representative of three separate experiments. *P<0.05, compared with control group. *1*: Normal; *2*: 50 μmol/L; *3*: 100 μmol/L; *4*: 200 μmol/L; *5*: 500 μmol/L.

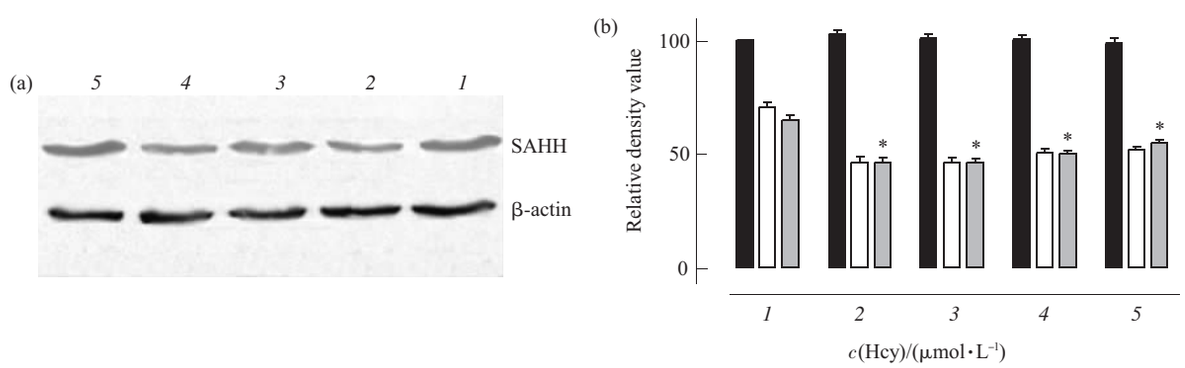

Fig. 4 Effects of homocysteine (Hcy) on SAHH protein levels in VSMCs

(a)Effects of Hcy on SAHH protein levels in HUVECs. HUVECs were incubated in the absence or presence of Hcy at various concentrations. The immunoblots were analyzed by densitometry. (b)The results were expressed as percentage of control ±*s* (error bar),each performed in duplicate. The control value was expressed as 100%. Related value was related to that of β-actin through the formula (related valve = experimentment densitometry value ×100/β-actin value). *P<0.05, compared with control group. ■:β-actin; □: SAHH experiment group; ▨: Related value. *1*: Control; *2*: 50 μmol/L; *3*: 100 μmol/L; *4*: 200 μmol/L; *5*: 500 μmol/L.

2.4 Endogenous C-5 DNA methyltransferase (C-5 MT-ase) activity

The endogenous C-5 DNA methyltransferase activity in homogenates of VSMCs is shown in Figure 5. Hcy up-regulates the activity of C-5 MT-ase, and its maximum activity was in 50 μmol/L Hcy concentration group ($P < 0.001$ compared with control group), and the other experimental groups also shows significant elevation of C-5 MT-ase activities ($P < 0.05$).

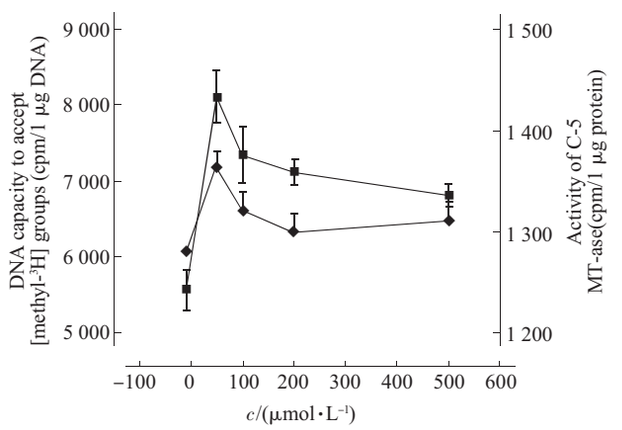

Fig. 5 Activity of C-5 MT-ase and gDNA capacity to accept methyl groups in different Hcy concentration

Activity of C-5 MT-ase was expressed as the amount of incorporated [methyl-^{3}H] groups into poly [dI-dC]. poly [dI-dC], present in cell homogenates (cpm ×10^{3}per 1 μg protein). DNA methyl-accepting capacity was expressed as the amount of [methyl-^{3}H] groups incorporated into gDNA (cpm ×10^{3}per 0.5 μg DNA). The data were presented as the $\bar{x} \pm s$ for independent experiments with three simultaneous samples per each. ◆—◆: Activity of C-5 MT-ase; ■—■: DNA capacity.

2.5 Methyl-accepting capacity of undigestion gDNA

Figure 5 also showed that the amount of gDNA methylation sites, which were available for the *Sss* Ⅰ methylase in all Hcy-treated groups, increase significantly ($P < 0.001$), and in 50 μmol/L group, it reaches the highest hill point. The incorporation of [methyl-^{3}H] SAM into the gDNA was inversely proportional to the initial DNA methylation status, which means that the gDNA isolated from cells and exposed to homocysteine exhibited 1.46, 1.32, 1.28 and 1.22 times ($P < 0.05$) higher level of methyl acceptance than gDNA of Hcy-untreated cells. This result indicated a Hcy-induced demethylation process in gDNA, and the observed changes of the DNA methylation status of gDNA also showed a parallel pattern to the endogenous C-5 DNA methyltransferase activity.

2.6 DNA methylation-dependent restriction analysis

Methyl-accepting capacity of gDNA with the methylation-dependent restriction analysis can probe the Hcy-induced alteration in DNA methylation and its potential sequence-bias. Methylation-dependent restriction endonucleases, which recognize unmethylated cytosine, can cut certain specific CG sequences but not the methylated ^{m}CG. The *Hpa* Ⅱ, specific for C$^{\downarrow}$CGG sequences and *Bss*H Ⅱ for CpG islands (GC$^{\downarrow}$GCGC) are used in this experiment for investigating the Hcy-induced alteration in DNA methylation and its potential sequence-bias. Digestion with *Hpa* Ⅱ or *Bss*H Ⅱ restriction endonucleases results in a destruction of corresponding CG loci and loss of the potential methylation-accepting sites.

Figure 6 shows an increase of methyl-accepting capacity of gDNA without being digested by the restriction endonucleases in all concentrations of homocysteine-treated groups, which copied the same results in Figure 5. This was due to the homocysteine-induced hypomethylation, and hence more methylation-accepting sites exposed. With the digestion by methylation-dependent endonucleases, however, the methyl-accepting capacity of gDNA would decrease because of the destruction of corresponding CG loci by the endonucleases. In control group the methyl-accepting capacity of gDNA showed a little but not significant decline while in all homocysteine-treated groups, the decrease of the methyl-accepting capacity is significant. This decline indicated hypomethylation is induced by Hcy in gDNA. The greater decrease in methylation-accepting capacity was noted in groups with *Hpa*Ⅱ digestion, its reductions in methylation-accepting capacity was 70.1%, 41.7%, 46.1% and 25.5% (50 μmol/L, 100 μmol/L, 200 μmol/L, 500 μmol/L homocysteine respectively) compared with undigested DNA. While the methylation-accepting capacity in *Bss*H Ⅱ cutting groups, the declined just approximately 45.5%, 8.1%, 7.4% and 8.0% (50 μmol/L, 100 μmol/L, 200 μmol/L, 500 μmol/L homocysteine respectively) compared with undigested DNA.

The greater decrease in methylation-accepting capacity in methylation-dependent restriction analysis indicated a relative lower level of methylation because the methylation-dependent restriction endonucleases just cut the unmethylated cytosine. If the cytosine was originally methylated, the enzymes would not be of

impact on it. So the results with methylation-dependent restriction analysis indicated that the homocysteine treatment can induce an decreased methylation in VSMCs gDNA or hypomethylation. And this induced-hypomethylation has a sequence-bias for *Hpa* Ⅱ cutting loci, which means Hcy may preferentially induce demethylation in C↓CGG sequences but not in CpG islands. The homocysteine induced-demethylation also showed a highest effect in its concentration of 50 μmol/L.

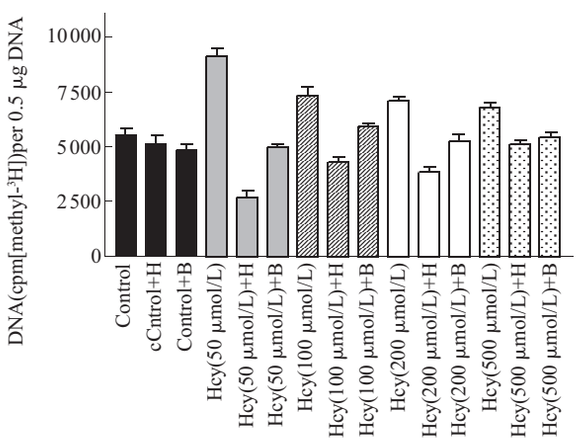

Fig. 6 Capacity of gDNA undigested and digested with *Hpa* Ⅱ (H) or *Bss*H Ⅱ (B) endonucleases to accept methyl groups after 24 h cell growth in the presence of the homocysteine

Each value, expressing the number of incorporated methyl groups into DNA(cpm×10³[methyl-³H]per 0.5 μg DNA), represents the $\bar{x}\pm s$ for six experiments with three simultaneous samples per each.

3 Discussion

Hyperhomocysteinemia is a common and independent risk factor for atherosclerosis [23]. The mechanisms of homocysteine (Hcy)-induced atherosclerosis have been incriminated to oxidative stress, apoptosis, inflammation etc, which is demonstrated by plenty of experimental evidence, but none is definitive so far. The chemical configuration of homocysteine posseses a reductive thio (—SH) group, which usually suggests anti-oxidative nature, as the cysteine does. The only difference between the two thio-containing amino- acids is the homocysteine has an extra —CH_2— group, as following: HS—CH_2—CH_2—$CHNH_2$—COOH for homocysteine and HS—CH_2—$CHNH_2$—COOH for cysteine. While the concentration of cysteine is about 20～25 times higher than that of homocysteine, it is usually not considered a risk factor for cardiovascular diseases[24]. Why did the homocysteine become a pro-oxidant and a famous risk factor for atherosclerosis? While the cysteine usually shows anti-oxidative nature. Many plausible explanations have not probe this key point of mechanisms.

The present results showed that an increased Hcy concentration induced elevated SAH, declined SAM and their ratio of SAM/SAH, reduced expression of SAH hydrolase, but increased activity of DNA MTase, the methylation status of gDNA was downgraded.

From the methionine cycle, the increased Hcy would feedback to inhibit the SAH hydrolase and a consequential accumulation of SAH. So a reduced expression of SAH hydrolase resulted from high Hcy concentration was easy to explain. But the result of increased activity of DNA MTase was unexpected, because the SAH was an inhibitor of many SAM-dependent methyl transferases (MTase). A potential, yet plausible expounding was the compensatory reaction of methylation machinery against homocysteine-induced hypomethylation. It has been reported from cancer tissue that MTase activity was actually increased in spite of the genome-wide hypomethylation [25], MTase activity can be seen as a compensatory mechanism to maintain genomic methylation pattern, since only two rounds of replications are required for genomic hypomethylation, if maintenance methylation activity provided by MTase or other methyl transferases was not operative. The decline of SAM could be resulted from excessive consumption due to increased activity of DNA MTase[26].

Analysis by methyl-accepting capacity of gDNA uncovers an increased methyl-accepting capacity after homocysteine treatment, which indicated a demethylation process in gDNA. In other words, the homocysteine caused hypomethylation in gDNA. Because the higher of the demethylation degree, the more of the methyl-acceptable loci[27].

With different methylation-dependent restriction endonucleases, the aberrant demethylation was found to prefer C↓CGG sequences to CpG islands. Methylation-dependent restriction endonucleases just cut the unmethylated cytosine. If the original methylated cytosine was demethylated by homocysteine treatment, the demethylated cytosine could be cut by endonucleases, and the methyl-accepting capacity would be lost in these locis

by endonucleases treatment. A smaller decline of methyl-accepting capacity after homocysteine treatment in *Bss*HⅡ than *Hpa*Ⅱ restriction analysis indicated a relative lower level of demethylation in sequence of *Bss*HⅡ cutting loci, which recognizes the CpG islands (GC↓GCGC). While in *Hpa*Ⅱ group, the loss of methyl-accepting capacity, treated by *Hpa*Ⅱ endonuclease, was much greater than in *Bss*HⅡ, because a higher demethylation induced by homocysteine treatment in *Hpa*Ⅱ recognizing loci would leave more unmethylated cytosines for *Hpa*Ⅱ cutting, so methyl-accepting capacity was lost during *Hpa*Ⅱ restriction analysis.

The current results strongly suggested that homocysteine treatment could lead hypomethylation of global DNA in VSMCs[28], and this demethylation was preferentially biased for C↓CGG sequence, not the CpG islands[29]. Although the CpG island was found to be more closely associated with promoters of many genes, the aberrant methylation patterns in non-CpG island sequence induced by homocystein may also deeply influence the expression of genes including the atherosclerosis-related genes, because maintenance of differential chromatin structure between transcriptionally competent, insulator and repressed genes were all critical aspects for transcriptional regulation.

The dosage of homocysteine used in the present studies clinically relevant from moderate hyperhomocysteinemia (Hcy concentration of 50 μmol/L, which is found in up to 40% of patients with myocardial infarction, stroke, or venous thrombosis) to severe hyperhomocysteinemia (Hcy concentration of 500 μmol/L, which is found in patients with inherited homocystinuria). The impacts of various concentration of homocysteine on the one-carbon methyl-group transferring metabolism, however, didn't show dose-effect relationship. The highest effects on aberrant methylation of gDNA and the factors involved in the pathway of DNA methylation and the SAM recycle were in the Hcy concentration of 50 μmol/L, an even increased Hcy concentrations, on the contrary, exert weaker effects on the aberrant methylation of gDNA and involved factors, which was unexpected, but may be reasonable. The hyperhomocysteinemia has been found associated with many deleterious effects, including pro-apoptosis on endothelial cells, promoting proliferation of vascular SMC, inducing oxidative stress, interfering NO bioactivity, activating some inflammatory pathway and coagulation cascade, even mediating cholesterol dysregulation etc. The higher concentration than 50 μmol/L may exert more direct injurious effects such as oxidative stress, apoptosis while the moderate hyperhomocysteinemia may show milder impact on epigenetic modulation of gene expression[30]. So the SMC shows a proliferation (see Figure 1) in Hcy concentration of 50 μmol/L, but a progressive reduced viable cell counts in Hcy concentration of 100 μmol/L and above. This phenomenon suggested that the varied detrimental effects of Hcy could be attributed to different concentrations via different mechanisms, in mild and moderate hyperhomocysteinemia, Hcy may primarily influence the epigenetic regulation of gene expression through the interference of methyl-group transferring metabolism while in more higher Hcy concentration, the essential impacts may be more directly injurious via oxidative stress, pro-apoptosis, inflammation etc.

Our findings uncovered a Hcy-induced hypomethylation in gDNA of vSMC, but a increased activity of DNA MTase, which was similar with the fact in cancer tissues. It is possible that alterations in DNA methylation may play an important role in atherogenesis, although it didn't prove a direct relationship between global hypomethylation and atherogenesis, but simply describe an association between these two processes. Our results also indicated a sequence bias in Hcy-induced hypomethylation for C↓CGG, but rather than for CpG island. And suggested that different concentrations of Hcy may exert different effects via different mechanisms. So the interventions directed towards hyperhomocysteine should be more specific according to the different concentrations and mechanisms in the treatment for vascular disorders. The induction of DNA methylation by HHcy is a new, hitherto unreported element of their mechanisms and these findings reveal a novel role of Hcy in the pathogenesis of human vascular disease.

References

1 Turhan H, Erbay A R, Yasar A S, *et al*. Plasma homocysteine levels in patients with isolated coronary artery ectasia. Int J Cardiol, 2005, **104** (2):158～162

2 van den Brandhof W E, Haks K, Schouten E G, *et al*. The relation between plasma cysteine, plasma homocysteine and coronary atherosclerosis. Atherosclerosis, 2001, **157** (2): 403～409

3 Duell P B, Malinow M R. Homocyst(e)ine: an important risk factor

for atherosclerotic vascular disease. Curr Opin Lipidol, 1997, **8** (16): 28～34

4 Refsum H, Ueland P M, Nygard O, *et al*. Homocysteine and cardiovascular disease. Annu Rev Med, 1998, **4** (9): 31～62

5 Ylä-Herttuala S, Nikkari T, Hirvonen J, *et al*. Biochemical composition ofcoronary arteries in Finnish children. Arteriosclerosis, 1986, **118** (6): 230～236

6 Viles-Gonzalez J F, Anand S X, Valdiviezo C, *et al*. Update in atherothrombotic disease. Mt Sinai J Med, 2004, **71** (3): 197～208

7 Feinberg A P, Tycko B. The history of cancer epigenetics. Nat Rev Cancer, 2004, **45** (4): 143～153

8 Greger V, Passarge E, Hopping W, *et al*. Epigenetic changes may contribute to the formation and spontaneous regression of retinoblastoma. Hum Genet, 1989, **83** (2): 155～158

9 Bestor T H, Tycko B. Creation of genomic methylation patterns. NatGenet, 1996, **12** (4): 363～367

10 Esteller M. CpG island methylation and histone modifications: biology and clinical significance. Ernst Schering Res Found Workshop, 2006, (57): 115～126

11 Jones P A, Laird P W. Cancer epigenetics comes of age. Nat Genet, 1999, **21**(2): 163～167

12 Hiltunen M O, Turunen M P, Hakkinen T P, *et al*. DNA ypomethylation and ethyltransferase expression in atherosclerotic lesions.Vasc Med, 2002, **7** (1): 5～11

13 Laukkanen M O, Mannermaa S, Hiltunen M O, *et al*. Local hypomethylation in atherosclerosis found in rabbit ec-sod gene. Arterioscler Thromb Vasc Biol, 1999, **19** (9): 2171～2178

14 Post W S, Goldschmidt-Clermont P J, Wilhide C C, *et al*. Methylation of the estrogen receptor gene is associated with aging and atherosclerosis in the cardiovascular system. Cardiovasc Res, 1999, **43** (55): 985～991

15 Laukkanen M O, Mannermaa S, Hiltunen M O, *et al*. Local hypomethylation in atherosclerosis found in rabbit ec-sod gene. Arterioscler Thromb Vasc Biol, 1999, **19** (9): 2171～2178

16 Ying A K, Hassanain H H, Roos C M, *et al*. Methylation of the estrogen receptor-alpha gene promoter is selectively increased in proliferating human aortic smooth muscle cells. Cardiovasc Res, 2000, **46** (1): 172～179

17 Audubert F, Breton M, Colard O, *et al*. Differential methylation patterns in molecular species of phosphatidylethanolamine derivatives in rat liver membranes. Biochim Biophys Acta, 1989, **1002** (1): 62～68

18 Strickler H D, Viscidi R, Escoffery C, *et al*. Adeno-associated virus and development of cervical neoplasia. J Med Virol, 1999, **59**(1): 60～65

19 Adams R L, Rinaldi A, Seivwright C. Microassay for DNA methyltransferase. J Biochem Biophys Methods, 1991, **22** (5): 19～22

20 Pogribny I, Yi P, James S J. A sensitive new method for rapid detection of abnormal methylation patterns in global DNA and within CpG islands. Biochem Biophys Res Commun, 1999, **262** (6): 624～628

21 Wyczechowska D, Fabianowska-Majewska K. The effects of cladribine and fludarabine on DNA methylation in K562 cells. Biochemical Pharmacology, 2003, **65** (6): 219～225

22 Pogribny I, Yi P, James S J, *et al*. A sensitive new method for rapid detection of abnormal methylation patterns in global DNA and within CpG islands. Biochem Biophys Res Commun, 1999, **262**(3): 624～628

23 Tsai J C, Perrella M A, Yoshizumi M. Promotion of vascular smooth muscle cell growth by homocysteine: a link to atherosclerosis. Proc Natl Acad Sci USA, 1994, **91** (14): 6369～6373

24 Haaf T. The effects of 5-azacytidine and 5-azadeoxycytidine on chromosome structure and function: implications for methylation-associated cellular processes. Pharmacol Ther, 1995, **65** (1):19～46

25 Lee P J, Washer L L, Law D J, *et al*. Limited up-regulation of DNA methyltransferase in human colon cancer reflecting increased cell proliferation. Proc Natl Acad Sci USA, 1996, **93** (19): 10366～10370

26 Issa J P, Vertino P M, Wu J, *et al*. Increased cytosine DNA-methyltransferase activity during colon cancer progression. J Natl Cancer Inst, 1993, **85** (15): 1235～1240

27 Andreassi M G, Botto N. DNA damage as a new emerging risk factor in atherosclerosis.Trends Cardiovasc Med, 2003, **13** (7): 270～275

28 White G P, Watt P M, Holt B J, *et al*. Differential patterns of methylation of the IFN-gamma promoter at CpG and non-CpG sites underlie differences in IFN-gamma gene expression between human neonatal and adult CD45RO-T cells. J Immunol, 2002, **168** (6): 2820～2827

29 Miniati P, Sourvinos G, Michalodimitrakis M, *et al*. Loss of heterozygosity on chromosomes 1, 2, 8, 9 and 17 in cerebral atherosclerotic plaques. Int J Biol Markers, 2001, **16** (3): 167～171

30 Counter C M, Avilion A A, LeFeuvre C E, *et al*. Telomere shortening associated with chromosome instability is arrested in immortal cells which express telomeraseactivity. EMBO J, 1992, **11** (6): 1921～1929

高半胱氨酸在平滑肌细胞中介导 DNA甲基化及机制的研究 *

姜怡邓[1)]　张建中[2)]　黄　英[1)]　苏　娟[1)]
张敬各[1)]　王丽珍[1)]　韩晓群[1)]　王树人[1)**]
([1)]四川大学华西医学中心基础与法医学院病理生理学教研室，成都 610041；
[2)]宁夏医学院基础学院病理学教研室，银川 750004)

摘要　高同型半胱氨酸血症是引起动脉粥样硬化一个重要独立的危险因子，可以引起基因 DNA 甲基化表型改变和蛋白质表达失调，但是基因甲基化表型改变的特点和动脉粥样硬化是否有关及其机制，到目前为止还没有研究清楚. 在平滑肌细胞培养的基础上研究高同型半胱氨酸血症对 DNA 甲基化的影响，高半胱氨酸诱导 DNA 甲基化表型改变的特征及潜在的机制. 高半胱氨酸加入人脐静脉平滑肌培养 24 h 后，高效液相检测 SAM 和 SAH 的浓度，实时 RT-PCR 和蛋白质印迹检测 SAH 水解酶 mRNA 和蛋白质表达. 通过内源性 DNA 甲基转移酶活性变化、基因组 DNA 接受甲基的能力、甲基化限制性内切酶分析检测 DNA 甲基化水平的变化. 结果显示，随着高半胱氨酸浓度的增加，SAH 水平增加，SAM 和 SAM/SAH 比率下降，SAH 水解酶水平下降，但 DNA 甲基转移酶活性增加，用不同甲基化限制性内切酶分析发现 C$^{\downarrow}$CGG 序列更容易甲基化. 由此可以推测，不同剂量的高半胱氨酸引起细胞损害效应的机制也不同，在低、中度高同型半胱氨酸血症，高半胱氨酸主要通过干扰高同型半胱氨酸的代谢途径影响基因表达表型修饰，在高度高同型半胱氨酸血症可能氧化应激、凋亡、炎症等发挥了更重要的作用.

关键词　高半胱氨酸，DNA 甲基转移酶，DNA 甲基化，SAM，SAH 水解酶
学科分类号　R965

---

*高等学校博士学科点专项科研基金项目(20050610050).
** 通讯联系人.
Tel: 028-85501268, E-mail: wangshuren1945@yahoo. com.cn
收稿日期：2006-10-23，接受日期：2006-12-06